 FDMP, vol.7, no.2, pp.175-199, 2011

Optimal Formulation of Nanofluids for Maximum Free Convection Heat Transfer from Horizontal Isothermal Cylinders

Massimo Corcione[1]

Abstract: Free convection heat transfer in nanofluids from horizontal isothermal cylinders is investigated theoretically. The main idea upon which the present work is based is that nanofluids behave more like a single-phase fluid rather than like a conventional solid-liquid mixture. This assumption implies that all the convective heat transfer correlations available in the literature for single-phase flows can be extended to nanoparticle suspensions, provided that the thermophysical properties appearing in them are the nanofluid effective properties calculated at the reference temperature. In this connection, two empirical equations, based on a wide variety of experimental data reported in the literature, are proposed for the evaluation of the nanofluid effective thermal conductivity and dynamic viscosity. Conversely, the other effective properties are computed by the traditional mixing theory. The heat transfer enhancement that derives from the dispersion of nano-sized solid particles into the base liquid is calculated for different operating conditions, nanoparticle diameters, and combinations of solid and liquid phases. The fundamental result obtained is the existence of an optimal particle loading for maximum heat transfer. In particular, for any assigned combination of suspended nanoparticles and base liquid, it is found that the optimal volume fraction increases as the nanofluid average temperature increases, the nanoparticle size decreases, and the Rayleigh number of the base fluid decreases.

Keywords: Nanofluids, Natural convection, Horizontal isothermal cylinders, Theoretical analysis, Optimal particle loading.

Nomenclature

c_p	specific heat at constant pressure
D	Einstein diffusion coefficient
d_f	equivalent diameter of a base fluid molecule

[1] DIAEE Area Fisica Tecnica, Sapienza Universita di Roma, via Eudossiana 18, 00184, Rome, Italy

d_p	nanoparticle diameter
E	heat transfer enhancement
h	coefficient of convection heat transfer
k	thermal conductivity
k_b	Boltzmann's constant = 1.38066×10^{-23} J/K
M	molecular weight of the base fluid
N	Avogadro number = 6.022×10^{23} mol^{-1}
Nu	Nusselt number
Pr	Prandtl number
Ra	Rayleigh number
Re	nanoparticle Reynolds number
T	temperature
u_B	nanoparticle Brownian velocity

Greek symbols

β	coefficient of thermal expansion
φ	nanoparticle volume fraction
μ	dynamic viscosity
ρ	mass density
τ_D	time required to cover a distance d_p moving at velocity u_B

Subscripts

eff	effective property
f	base fluid
fr	freezing point of the base liquid
max	maximum value
opt	optimal value
ref	reference state for the calculation of the thermophysical properties
s	solid phase
w	surface of the cylinder
∞	undisturbed fluid reservoir

1 Introduction

Buoyancy-induced convection is the cooling strategy preferred by heat transfer designers when a small power consumption, a negligible operating noise, and a high

reliability of the system, are main concerns. However, the intrinsic low thermal performance of natural convection, in comparison with equivalent or similar forced convection cases, is a substantial limitation – see e.g. the studies performed by El Alami, Semma, Najam and Boutarfa (2009), and Meskini, Najam and El Alami. A possible solution to mitigate the problem is the replacement of conventional coolants, such as water, ethylene glycol, and mineral oils, with nanofluids, i.e. liquid suspensions of nano-sized solid particles, whose effective thermal conductivity is known to be higher than that of the corresponding pure base liquid.

The majority of the papers available in the literature on convective heat transfer in nanofluids are related to forced convection flows, proving that nanoparticle suspensions have undoubtedly a great potential for heat transfer enhancement, as discussed in the review-articles recently compiled by Daungthongsuk and Wongwises (2007), Murshed, Leong and Yang (2008a), and Kakaç and Pramuanjaroenkij (2009). Conversely, the relatively few works performed on buoyancy-induced heat transfer in nanofluids, most of which are numerical studies dealing with enclosed flows, lead to contradictory conclusions, leaving still unanswered the question if the use of nanoparticle suspensions for natural convection applications is actually advantageous with respect to pure liquids. In fact, according to some authors, the addition of nanoparticles to a base liquid implies a more or less remarkable enhancement of the heat transfer rate, whilst, according to others, a deterioration may occur.

The reason for such conflicting results can be explained by considering that the heat transfer performance of nanofluids in natural convection flows is a strict consequence of the two opposite effects arising from the increase of the effective thermal conductivity and the increase of the effective dynamic viscosity that occur as the nanoparticle volume fraction is augmented. In other words, the dispersion of a certain concentration of nanoparticles into a base liquid can bring to either an enhancement or a degradation of the heat transfer performance in buoyancy-induced flows, depending on whether the increased thermal conductivity effect is larger or smaller than the increased viscosity effect. Now, the typical approach used to investigate the main heat transfer features of nanoparticle suspensions is based on the assumption that nanofluids behave more like a single-phase fluid rather than a conventional solid-liquid mixture, which means that the mass, momentum and energy transfer governing equations for pure fluids can be directly extended to nanoparticle suspensions, provided that the thermophysical properties appearing in them are the nanofluid effective properties. Therefore, the use of robust models, capable to predict the nanofluid effective thermal conductivity and dynamic viscosity as more accurately as possible, is crucial for obtaining realistic data. Unfortunately, almost all the numerical studies available in the literature on buoyancy-driven nanofluids

miss this requirement, thus leading to unreliable conclusions. Actually, one of the commonest reasons behind erroneous results is the use of the Einstein equation [Einstein (1906, 1911)] or the Brinkman equation [Brinkman (1952)] for calculating the effective dynamic viscosity of nanofluids, whose values are notoriously underestimated by these models. Moreover, the effective thermal conductivity is often evaluated by the Maxwell-Garnett model [Maxwell-Garnett (1904)] or other traditional mean-field theories, such as the Bruggeman model [Bruggemann (1935)] and the Hamilton−Crosser model [Hamilton and Crosser (1962)], that appear to be suitable to this end when the nanofluid is at "room" temperature − see e.g. Eapen, Williams, Buongiorno, Hu, Yip, Rusconi and Piazza (2007), and Buongiorno et al. (2009) −, but fail dramatically when the temperature of the suspension is one or some tens degrees higher than 20−25°C, as e.g. shown in Das, Putra, Thiesen and Roetzel (2003), Li and Peterson (2006), and Yu, Xie, Chen and Li (2010).

Framed in this general background, the aim of the present paper is to undertake a comprehensive theoretical study on natural convection heat transfer from a long horizontal isothermal cylinder suspended in a nanofluid, that is a topic never investigated before, with the primary scope to determine the main heat transfer features for different operating conditions, nanoparticle diameters, and solid-liquid combinations.

2 Theoretical formulation of the problem

Although strictly speaking a nanofluid is a solid-liquid mixture, the approach conventionally used in most studies on this subject handles the nanofluid as a single-phase fluid. In fact, since the suspended nanoparticles have usually small size and concentration, the hypothesis of a solid-liquid mixture statistically homogeneous and isotropic can reasonably be advanced. This means that, under the further assumptions that the nanoparticles and base liquid are in local thermal equilibrium, and no slip motion occurs between the solid and liquid phases, to all intents and purposes the nanofluid can be treated as a pure fluid. Therefore, all the convective heat transfer correlations available in the literature for single-phase flows can easily be extended to the corresponding nanofluid applications, provided that the thermophysical properties appearing in them are the nanofluid effective properties calculated at the reference temperature. Notice that a similar approach was previously used by Kim, Kang and Choi (2004), and Hwang, Lee and Jang (2007), for investigating the Rayleigh-Bénard convection of nanofluids, and later by Corcione (2010) for studying the main heat transfer features of buoyancy-driven nanofluids inside rectangular enclosures differentially heated at the vertical walls.

For natural convection heat transfer occurring between a long horizontal cylinder at uniform temperature T_w and the surrounding undisturbed fluid reservoir at tem-

perature T_∞, the Churchill−Chu correlation [Churchill and Chu (1975)], based on a wide number of experimental data obtained from other authors, is usually recommended − see e.g. Bejan (2004), Martynenko and Khramtsov (2005), and Incropera, DeWitt, Bergman and Lavine (2007):

$$Nu^{1/2} = 0.60 + \frac{0.387Ra^{1/6}}{\left[1+\left(\frac{0.559}{\mathrm{Pr}}\right)^{9/16}\right]^{8/27}} \quad Ra \leq 10^{13} \tag{1}$$

where the characteristic length in the Nusselt and Rayleigh numbers is the cylinder diameter, and the physical properties are evaluated at the reference temperature T_{ref} = $(T_w + T_\infty)/2$.

The Churchill-Chu heat transfer correlation expressed by eq. (1) will then be used to assess the effect of the nanoparticle volume fraction on the heat transfer enhancement, E, defined as

$$\mathrm{E} = \frac{h_{eff}}{h_f} - 1 = \frac{Nu_{eff}}{Nu} \times \frac{k_{eff}}{k_f} - 1, \tag{2}$$

where h_f, k_f and Nu are the coefficient of convection, the thermal conductivity and the Nusselt number of the base fluid, respectively, and h_{eff}, k_{eff} and Nu_{eff} are the corresponding effective quantities of the nanoparticle suspension. Recall that Nu_{eff} is the outcome of eq. (1) in which the Rayleigh and Prandtl numbers of the pure fluid are replaced by the effective Rayleigh and Prandtl numbers of the nanofluid calculated at the reference temperature T_{ref}.

3 Nanofluid effective thermophysical properties

3.1 Effective thermal conductivity

The inadequacy of the traditional mean-field theories in predicting the effective thermal conductivity of nanofluids has motivated the development of several new models. A wide number of these models account for the effects of the phenomena occurring at the solid/liquid interface and/or the micro-mixing convection caused by the Brownian motion of the suspended nanoparticles – see e.g. Yu and Choi (2003), Xue (2003), Kumar, Patel, Kumar, Sundararajan, Pradeep and Das (2004), Koo and Kleinstreuer (2004), Jang and Choi (2004), Xie, Fujii and Zhang (2005), Patel, Sundararajan, Pradeep, Dasgupta, Dasgupta and Das (2005), Ren, Xie and Cai (2005), Prasher, Bhattacharya and Phelan (2005, 2006), Leong, Yang and Murshed (2006), Xuan, Li, Zhang and Fujii (2006), Prakash and Giannelis (2007), and Murshed, Leong and Yang (2009). Other models account for the nanoparticle aggregation that causes local percolation effects − see e.g. Wang, Zhou and Peng

(2003), Prasher, Evans, Meakin, Fish, Phelan and Keblinski (2006), and Evans, Prasher, Fish, Meakin, Phelan and Keblinski (2008) – or combine the micro-convection due to the Brownian motion and the aggregation occurring among individual nanoparticles and/or nanoparticle clusters – see e.g. Xuan, Li and Hu (2003), and Prasher, Phelan and Bhattacharya (2006). However, these models show large discrepancies among each other, which clearly represents a restriction to their applicability. Moreover, many of them include empirical constants of proportionality whose values were often determined on the basis of a limited number of experimental data, or were not clearly defined.

Hence, an empirical correlation based on a wide variety of experimental data available in the literature has been developed for k_{eff}/k_f. In this regard, it is worth pointing out that a certain dispersion of the experimental data reported by different authors for the same type of nanofluid is unavoidable. Indeed, in some cases the discrepancies among the data may reach the order of 50%, which could be due to the different measurement techniques used in experiments, as well as to the different degrees of dispersion/agglomeration obtained for the suspended nanoparticles, and the accuracy of evaluation of their shape and size. Therefore, in deriving the correlation proposed here and used for computations, some data-sets found in the literature have been discarded because either the data were in a too sharp contrast with the main body of the available results without any convincing physical evidence, or the investigation procedure was not properly described in detail, or specific chemical dispersants/surfactants were used in experiments, which could have significantly altered the thermo-mechanical behaviour of the suspension. The experimental data upon which the correlation is based are extracted from the following sources: Masuda, Ebata, Teramae and Hishinuma (1993) for TiO_2(27 nm) + H_2O; Pak and Cho (1998) for TiO_2(27 nm) + H_2O; Lee, Choi, Li and Eastman (1999) for CuO(23.6 nm) + H_2O, CuO(23.6 nm) + ethylene glycol (EG), Al_2O_3(38.4 nm) + H_2O, and Al_2O_3(38.4 nm) + EG; Eastman, Choi, Li, Yu and Thompson (2001) for Cu(10 nm) + EG; Das, Putra, Thiesen and Roetzel (2003) for CuO(28.6 nm) + H_2O, and Al_2O_3(38.4 nm) + H_2O; Chon, Kihm, Lee and Choi (2005) for Al_2O_3(47 nm) + H_2O; Chon and Kihm (2005) for Al_2O_3(47 nm and 150 nm) + H_2O; Xuan, Li, Zhang and Fujii (2006) for TiO_2(27 nm) + H_2O; Murshed, Leong and Yang (2008b) for Al_2O_3(80 nm) + H_2O, and Al_2O_3(80 nm) + EG; Mintsa, Roy, Nguyen and Doucet (2009) for CuO(29 nm) + H_2O; and Duangthongsuk and Wongwises (2009) for TiO_2(21 nm) + H_2O. The nanoparticle volume fraction and the nanofluid temperature lie in the ranges between 0.002 and 0.09, and between 294 K and 324 K, respectively.

By way of regression analysis, the following mean empirical correlation with a

1.86% standard deviation of error and a ± 4% range of error is produced:

$$\frac{k_{eff}}{k_f} = 1 + 4.4Re^{0.4}\,\mathrm{Pr}^{0.66}\left(\frac{T}{T_{fr}}\right)^{10}\left(\frac{k_s}{k_f}\right)^{0.03}\varphi^{0.66}, \tag{3}$$

where Re is the nanoparticle Reynolds number, Pr is the Prandtl number of the base liquid, T is the nanofluid temperature, T_{fr} is the freezing point of the base liquid, k_s is the thermal conductivity of the solid nanoparticles, and φ is the nanoparticle volume fraction. The Reynolds number of the suspended nanoparticles is defined as $\mathrm{Re} = (\rho_f u_B d_p)/\mu_f$, where ρ_f and μ_f are the mass density and dynamic viscosity of the base fluid, respectively, and d_p and u_B are the nanoparticle diameter and the nanoparticle Brownian velocity, respectively. Once u_B is calculated as the ratio between d_p and the time required to cover such a distance $\tau_D = (d_p)^2/6D$ – see Keblinki, Phillpot and Choi (2002) –, in which D stands for the Einstein diffusion coefficient, the nanoparticle Reynolds number is given by

$$Re = \frac{2\rho_f k_b T}{\pi \mu_f^2 d_p}, \tag{4}$$

where $k_b = 1.38066\times10^{-23}$ J/K is the Boltzmann's constant. Notice that in eqs. (3) and (4) all the physical properties are calculated at the nanofluid temperature T.

It is apparent that the dimensionless effective thermal conductivity of the nanofluid, k_{eff}/k_f, increases as φ and T increase, and d_p decreases. Moreover, k_{eff}/k_f depends marginally on the solid-liquid combination, as denoted by the extremely small exponent of the particle-fluid thermal conductivity ratio.

Although the mechanisms behind the thermal behaviour of nanofluids are still in debate, a tentative conclusion may be reached on the basis of the observations reported above. In fact, since the data used to derive eq. (3) are relative to solid-liquid combinations having a thermal conductivity ratio k_s/k_f that spans over two orders of magnitude (from nearly 15 for TiO_2 + H_2O to more than 1500 for Cu + EG), the substantial independence of k_{eff}/k_f from k_s/k_f gives strength to the possibility that the Brownian motion of the suspended nanoparticles plays a non-negligible role. Of course, when the nanoparticle concentration increases, the chance that the nanoparticles aggregate forming complex massive clusters gets progressively higher, which has the consequence that the contribution of the Brownian motion to the enhanced thermal conductivity tends inevitably to decrease. However, at same time, the contribution of the percolation behavior increases. In this regard, the fact that the growth of k_{eff}/k_f with φ occurs with a decreasing slope, as reflected by the 0.66 exponent of φ in eq. (3), may suggest the hypothesis that percolation is a heat transport mechanism proportionally less effective than micro-convection.

The distributions of k_{eff}/k_f vs. φ that emerge from eq. (3) for Al_2O_3 + H_2O, with d_p and T as parameters, are displayed in Fig. 1, where the prediction of the Maxwell-Garnett equation is also reported for comparison, showing that the degree of failure of this model applied to nanofluids increases as the temperature increases, and the nanoparticle size decreases.

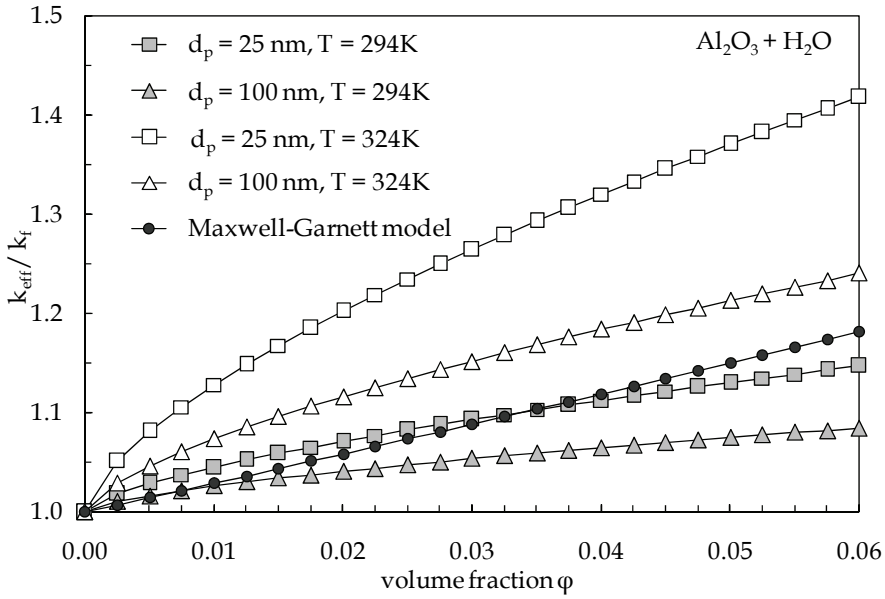

Figure 1: Distributions of k_{eff}/k_f vs. φ for Al_2O_3+ H_2O, with d_p and T as parameters.

3.2 Effective dynamic viscosity

Although the traditional theories underpredict significantly the effective dynamic viscosity of nanofluids, only few models have recently been proposed for describing the rheological behaviour of nanofluids, such as those developed by Koo (2005), Masoumi, Sohrabi and Behzadmehr (2009), and Ganguly and Chakraborty (2009). However, as these models contain empirical correction factors based on an extremely small number of experimental data, their regions of validity are someway limited.

Therefore, an empirical correlation based on a large number of experimental data selected from literature has been developed for μ_{eff}/μ_f, where μ_{eff} is the effective dynamic viscosity of the nanofluid, and μ_f is the dynamic viscosity of the base

fluid. Of course, the considerations stated earlier about the dispersion of the thermal conductivity data available in the literature apply also to the dynamic viscosity. The experimental data used to construct the correlation proposed here are taken out of the following sources: Masuda, Ebata, Teramae and Hishinuma (1993) for TiO_2(27 nm) + H_2O; Pak and Cho (1998) for TiO_2(27 nm) + H_2O; Wang, Xu and Choi (1999) for Al_2O_3(28 nm) + H_2O; Putra, Roetzel and Das (2003), and Das, Putra and Roetzel (2003) for Al_2O_3(38 nm) + H_2O; Prasher, Song, Wang and Phelan (2006) for Al_2O_3(27 nm, 40 nm, and 50 nm) + propylene glycol (PG); He, Jin, Chen, Ding, Cang and Lu (2007) for TiO_2(95 nm) + H_2O; Chen, Ding and Tan (2007) and Chen, Ding, He and Tan (2007) for TiO_2(25 nm) + ethylene glycol (EG); Chevalier, Tillement and Ayela (2007) for SiO_2(35 nm, 94 nm, and 190 nm) + ethanol; Lee, Hwang, Jang, Lee, Kim, Choi and Choi (2008) for Al_2O_3(30 nm) + H_2O; and Garg, Poudel, Chiesa, Gordon, Ma, Wang, Ren, Kang, Ohtani, Nanda, McKinley and Chen (2008) for Cu(200 nm) + EG. The nanoparticle volume fraction and the nanofluid temperature lie in the ranges between 0.0001 and 0.071, and between 293 K and 323 K, respectively.

By way of regression analysis, the following mean empirical correlation with a 1.84% standard deviation of error and a $\pm$ 4.5% range of error is obtained:

$$\frac{\mu_{eff}}{\mu_f} = \frac{1}{1 - 34.87(d_p/d_f)^{-0.3}\varphi^{1.03}}, \tag{5}$$

where d_f is the equivalent diameter of a base fluid molecule, given by

$$d_f = 0.1 \left[\frac{6M}{N\pi\rho_{f0}}\right]^{1/3}, \tag{6}$$

in which M is the molecular weight of the base fluid, N is the Avogadro number, and ρ_{f0} is the mass density of the base fluid calculated at temperature T_0 = 293 K.

It may be observed that, within the approximation of eq. (5), μ_{eff}/μ_f is independent of both the solid-liquid combination and the temperature, at least for particle volume fractions not too high and temperatures not too far from "room" temperature. Another interesting feature is that μ_{eff}/μ_f increases as d_p decreases and φ increases. This can tentatively be explained if we reasonably assume that the dynamic viscosity of a nanofluid is somehow related to the amount of friction occurring at the contact surface between nanoparticles and base liquid, and to the strength of the colloidal interactions and the degree of aggregation existing among the suspended nanoparticles. The amount of friction between nanoparticles and base fluid depends on the wideness of the overall contact surface, whose area, for an assigned volume fraction, is inversely proportional to the nanoparticle diameter.

On the other hand, fixed the nanoparticle diameter, both the strength of the colloidal interactions and the degree of aggregation are expected to increase with increasing the nanoparticle concentration.

As an example, the distributions of μ_{eff}/μ_f vs. φ that emerge from eq. (5) for different values of d_p are displayed in Fig. 2, where the predictions of the Brinkman equation (that are practically identical to those of the Einstein equation) are additionally delineated, pointing out that the error deriving from its application to nanofluids increases remarkably with decreasing the nanoparticle size.

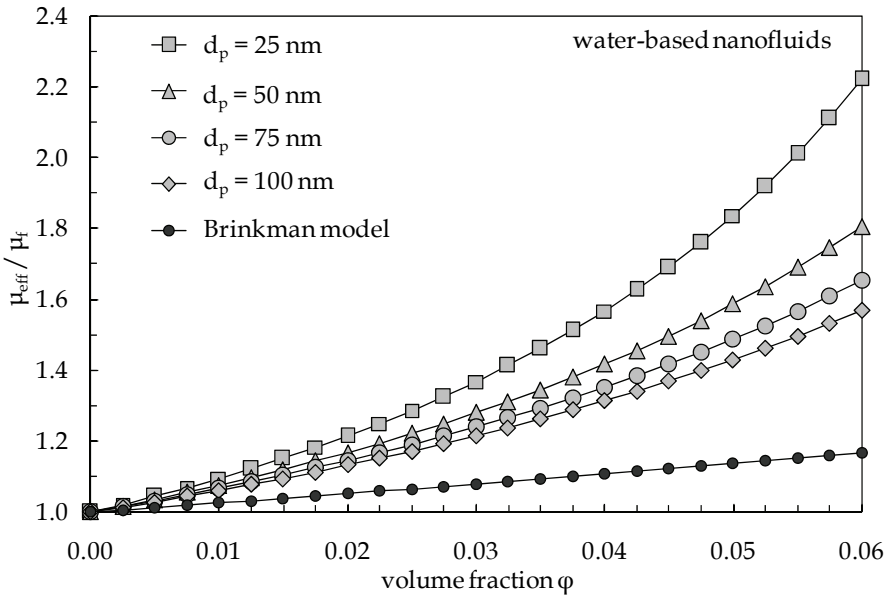

Figure 2: Distributions of μ_{eff}/μ_f vs. φ for water-based nanofluids, with d_p as a parameter.

3.3 Other effective physical properties

The other effective physical properties of the nanofluid are calculated according to the mixing theory, as typically done in the majority of the studies performed in this field.

The effective mass density of the nanofluid, ρ_{eff}, is given by

$$\rho_{eff} = (1-\varphi)\rho_f + \varphi\rho_s, \tag{7}$$

where ρ_f and ρ_s are the mass densities of the base fluid and the solid nanoparticles, respectively.

The heat capacity per unit volume of the nanofluid, $(\rho c_P)_{eff}$, is

$$(\rho c_P)_{eff} = (1-\varphi)(\rho c_P)_f + \varphi(\rho c_P)_s, \tag{8}$$

where c_p is the specific heat at constant pressure, and $(\rho c_p)_f$ and $(\rho c_p)_s$ are the heat capacities per unit volume of the base fluid and the solid nanoparticles, respectively. Accordingly, the effective specific heat at constant pressure of the nanofluid, $(c_P)_{eff}$, is calculated as

$$(c_P)_{eff} = \frac{(1-\varphi)(\rho c_P)_f + \varphi(\rho c_P)_s}{(1-\varphi)\rho_f + \varphi\rho_s}. \tag{9}$$

The effective coefficient of thermal expansion of the nanofluid, β_{eff}, is defined by

$$(\rho\beta)_{eff} = -\frac{d\rho_{eff}}{dT}. \tag{10}$$

If we substitute eq. (7) into eq. (10), and replace the temperature derivatives of ρ_f and ρ_s with $(\rho\beta)_f$ and $(\rho\beta)_s$, respectively, we have

$$(\rho\beta)_{eff} = (1-\varphi)(\rho\beta)_f + \varphi(\rho\beta)_s, \tag{11}$$

thus obtaining

$$\beta_{eff} = \frac{(1-\varphi)(\rho\beta)_f + \varphi(\rho\beta)_s}{(1-\varphi)\rho_f + \varphi\rho_s}. \tag{12}$$

The distributions of the dimensionless effective mass density, ρ_{eff}/ρ_f, the dimensionless effective specific heat at constant pressure, $(c_p)_{eff}/\ (c_p)_f$, and the dimensionless effective coefficient of thermal expansion, β_{eff}/β_f, plotted against the nanoparticle volume fraction for Al_2O_3 + H_2O at T = 309 K, are shown in Fig. 3, where the distributions of the dimensionless effective heat capacity per unit volume, $(\rho c_p)_{eff}/\ (\rho c_p)_f$, and the dimensionless effective temperature derivative of the mass density, $(\rho\beta)_{eff}/\ (\rho\beta)_f$, are also represented.

4 Results and discussion

The effect of the nanoparticle volume fraction on the heat transfer enhancement is calculated for different diameters of the suspended nanoparticles, average temperatures of the nanofluid, Rayleigh numbers of the base fluid, and for a number of combinations between solid and liquid phases.

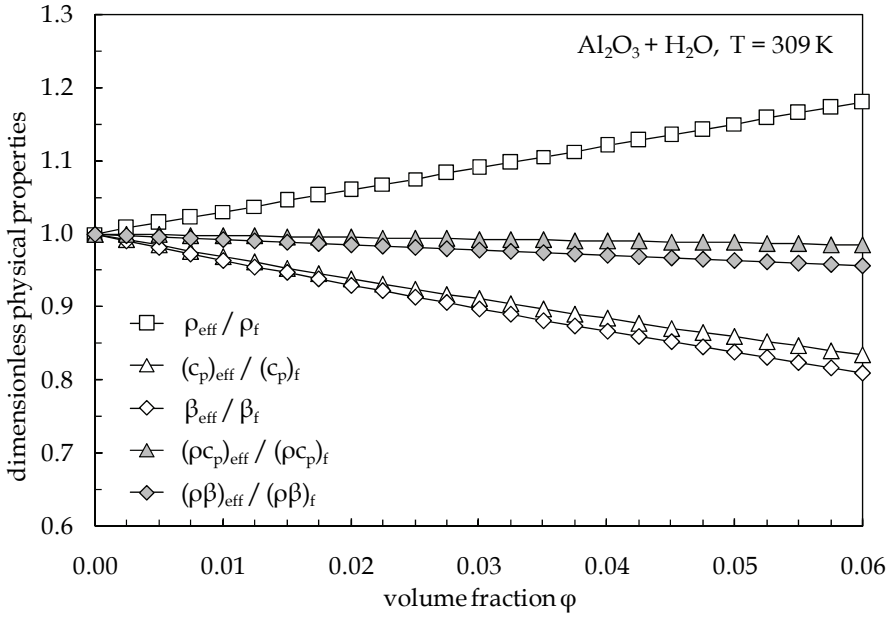

Figure 3: Distributions of the other dimensionless physical properties vs. φ for Al_2O_3+ H_2O at T = 309 K.

The results obtained for Al_2O_3 + H_2O are displayed and discussed first; subsequently, the results obtained for other solid-liquid mixtures are shown.

The effects of the size of the suspended nanoparticles and the nanofluid average temperature are pointed out in Figs. 4 and 5, where the distributions of the percentage heat transfer enhancement, E, are plotted versus the volume fraction, φ, for different nanoparticle diameters, and different average temperatures of the nanofluid, respectively. In the same figures, the distributions of E vs. φ obtained by using the Maxwell-Garnett and Brinkman models for calculating the effective thermal conductivity and dynamic viscosity of the nanofluid are also reported, confirming the weakness of these models in capturing the main features of the thermal and rheological behaviours of nanoparticle suspensions.

It may be seen that, owing to the dispersion of a progressively larger amount of nano-sized solid particles into the base liquid, the heat transfer enhancement increases up to a point, which is due to the increased effective thermal conductivity of the nanofluid. Notice that the impact of the increased effective thermal conductivity is higher when the diameter of the suspended nanoparticles is smaller and the nanofluid average temperature is higher. The value of φ corresponding to the peak

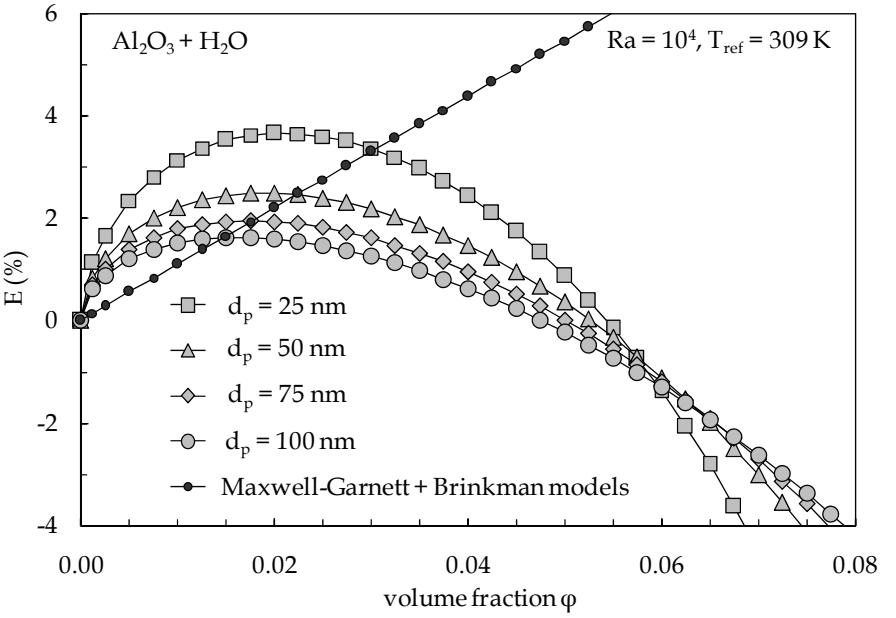

Figure 4: Distributions of E (%) vs. φ for Al_2O_3+ H_2O at Ra = 10^4 and T_{ref} = 309 K, with d_p as a parameter.

vskip2em

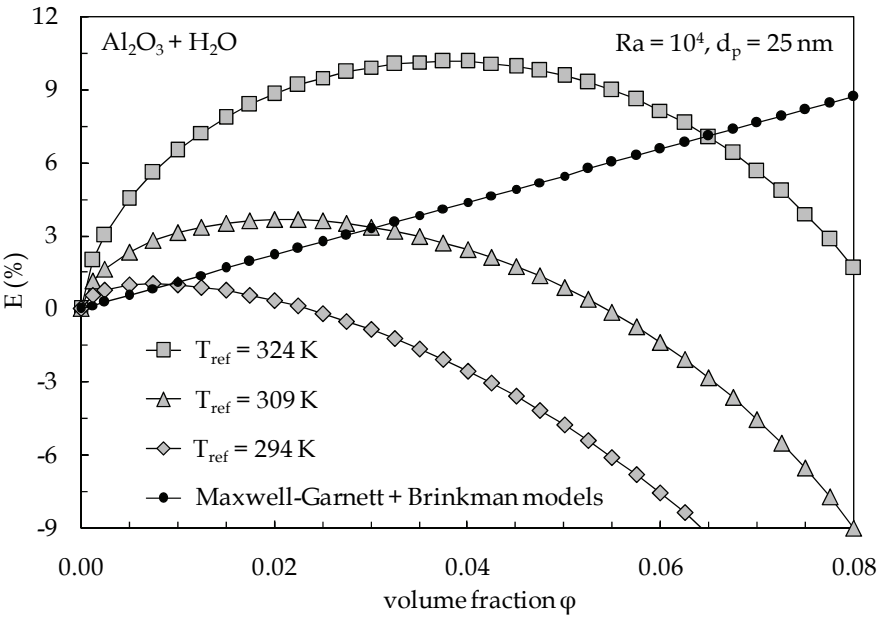

Figure 5: Distributions of E (%) vs. φ for Al_2O_3(d_p = 25 nm) + H_2O at Ra = 10^4, with T_{ref} as a parameter.

of E is defined as the optimal particle loading φ_{opt}. As the volume fraction is further increased above φ_{opt}, the heat transfer enhancement decreases, which is due to the excessive growth of the nanofluid effective viscosity. In fact, as discussed earlier, the nanofluid behaviour in natural convection flows is a consequence of the two opposite effects that originate from the increase of both the effective thermal conductivity and the effective dynamic viscosity occurring as the nanoparticle concentration increases. According to Figs. 1 and 2, the first effect, which tends to enhance the heat transfer performance, prevails at small volume fractions, whilst the second effect, which tends to degrade the heat transfer performance, prevails at large volume fractions. Obviously, when the increased viscosity effect outweighs the increased thermal conductivity effect, the heat transfer enhancement becomes negative, which means that the convective thermal performance of the nanofluid is lower than that of the pure base liquid.

Distributions of E vs. φ with same trend of those reported in Figs. 4 and 5 are obtained for any other investigated Rayleigh number of the base liquid, as displayed in Fig. 6. It is apparent that the smaller is the Rayleigh number of the base liquid, the more pronounced is the heat transfer enhancement produced by the addition of solid nanoparticles to the base liquid. In fact, at small Rayleigh numbers the flow is featured by a low heat and momentum transfer performance, which implies that the addition of nanoparticles to the base fluid results in an increased thermal conductivity effect that prevails upon the increased viscosity effect. On the contrary, at large Rayleigh numbers the flow is characterized by a high heat and momentum transfer performance, thus implying that the dispersion of nano-sized particles into the base fluid results in a more significant increased viscosity effect, that may even predominate upon the increased thermal conductivity effect, especially at high volume fractions, with a consequent deterioration of the heat transfer performance.

As far as the optimal particle loading is concerned, a set of distibutions of φ_{opt} vs. Ra are represented in Fig. 7 for different combinations of values of d_p and T_{ref}. It may be noticed that φ_{opt} depends very slightly on the nanoparticle size, whilst it increases notably as the nanofluid average temperature is increased. In fact, both k_{eff}/k_f and μ_{eff}/μ_f increase as d_p is reduced, which implies that the effect of the nanoparticle size on φ_{opt} is quite moderate. Conversely, owing that k_{eff}/k_f enhances significantly when T_{ref} is increased, whilst μ_{eff}/μ_f keeps constant, the nanoparticle concentration at which the increase in viscosity becomes excessive magnifies with increasing the nanofluid average temperature.

The distributions of the percentage heat transfer enhancement at the optimal particle loading, E_{max}, plotted versus the Rayleigh number of the base fluid, are reported in Figs. 8 and 9, for the same values of d_p and T_{ref} used in Fig. 7. Again, it is clear that the heat transfer enhancement consequent to the addition of nanoparticles to a

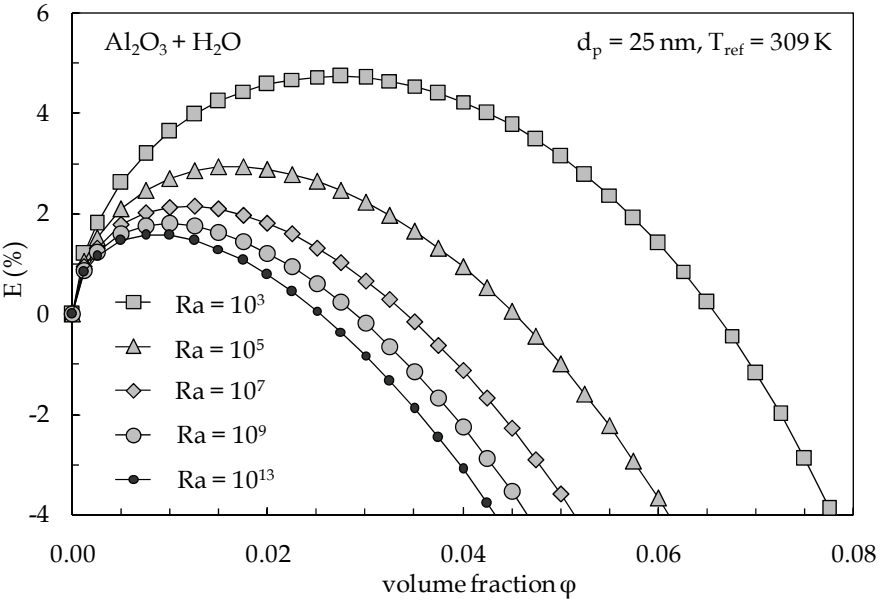

Figure 6: Distributions of E (%) vs. φ for Al_2O_3(d_p = 25 nm) + H_2O at T_{ref} = 309 K, with Ra as a parameter.

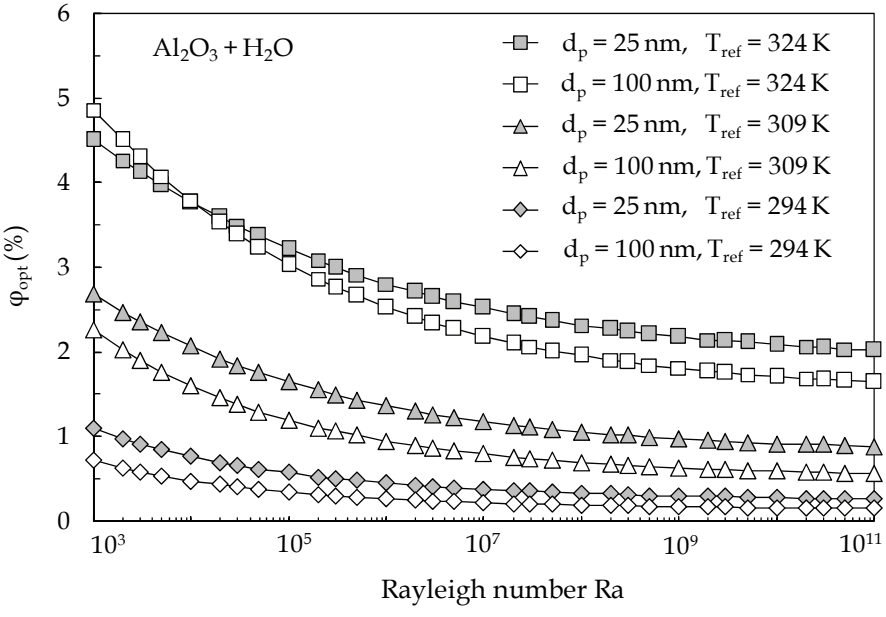

Figure 7: Distributions of $\varphi_{opt}(\%)$ vs. Ra for Al_2O_3+ H_2O, with d_p and T_{ref} as parameters.

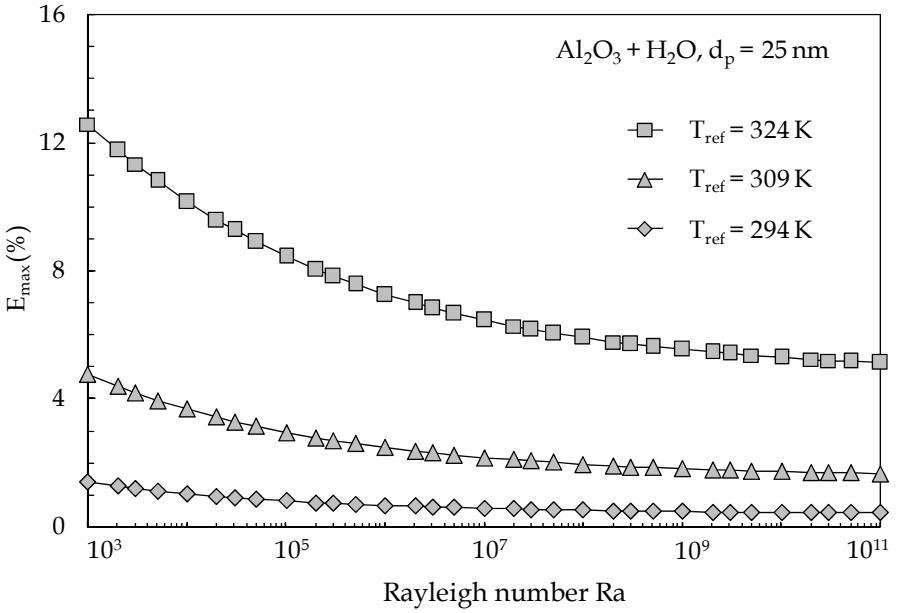

Figure 8: Distributions of $E_{max}(\%)$ vs. Ra for $Al_2O_3(d_p = 25$ nm) + H_2O, with T_{ref} as a parameter.

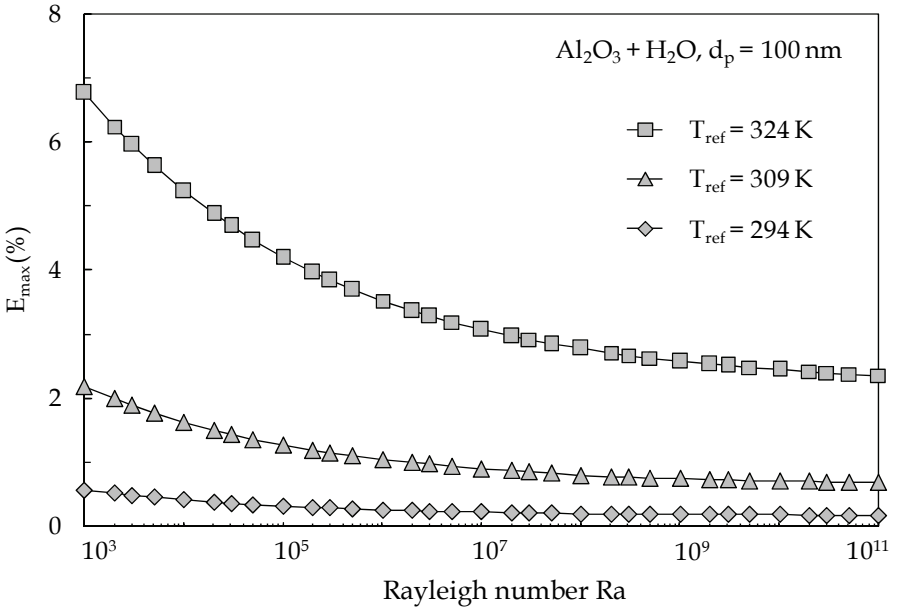

Figure 9: Distributions of $E_{max}(\%)$ vs. Ra for $Al_2O_3(d_p = 100$ nm) + H_2O, with T_{ref} as a parameter.

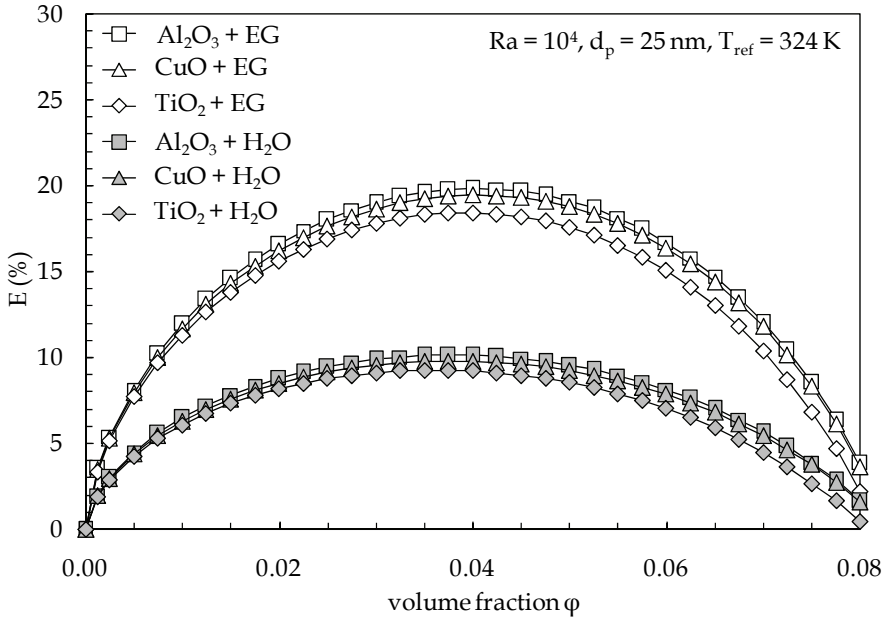

Figure 10: Distributions of E (%) vs. φ for different nanofluids, assumed Ra = 10^4, d_p = 25 nm and T_{ref} = 324 K.

base fluid is much more remarkable at small Rayleigh numbers rather than at large Rayleigh numbers of the base fluid.

Finally, the distributions of E versus φ for different solid-liquid combinations are plotted in Fig. 10, showing that the effect of the base fluid is more remarkable than that of the nanoparticle material. This can be justified by considering that, based on eq. (2), E depends on both Nu_{eff}/Nu and k_{eff}/k_f. From eq. (1), if we take into account that for many liquids the Prandtl number is generally much larger than 0.559, we derive that Nu_{eff}/Nu is a primary function of Ra_{eff}/Ra, which is equal to the ratio of the product $[(\rho\beta)_{eff}/(\rho\beta)_f] \times [(\rho c_p)_{eff}/(\rho c_p)_f]$ to the product $(k_{eff}/k_f) \times (\mu_{eff}/\mu_f)$. On the other hand, according to Fig. 3, both $(\rho\beta)_{eff}/(\rho\beta)_f$ and $(\rho c_p)_{eff}/(\rho c_p)_f$ remain practically constant with increasing φ. This means that the heat transfer enhancement, E, depends mostly on the dimensionless effective thermal conductivity, k_{eff}/k_f, and the dimensionless effective dynamic viscosity, μ_{eff}/μ_f. Hence, owing that k_{eff}/k_f depends very few on the nanoparticle material, whereas μ_{eff}/μ_f is completely independent of the nanoparticle material, we can conclude that E is affected much more by the liquid phase than by the solid phase. Obviously, since the thermal conductivity of water is more than the double of the

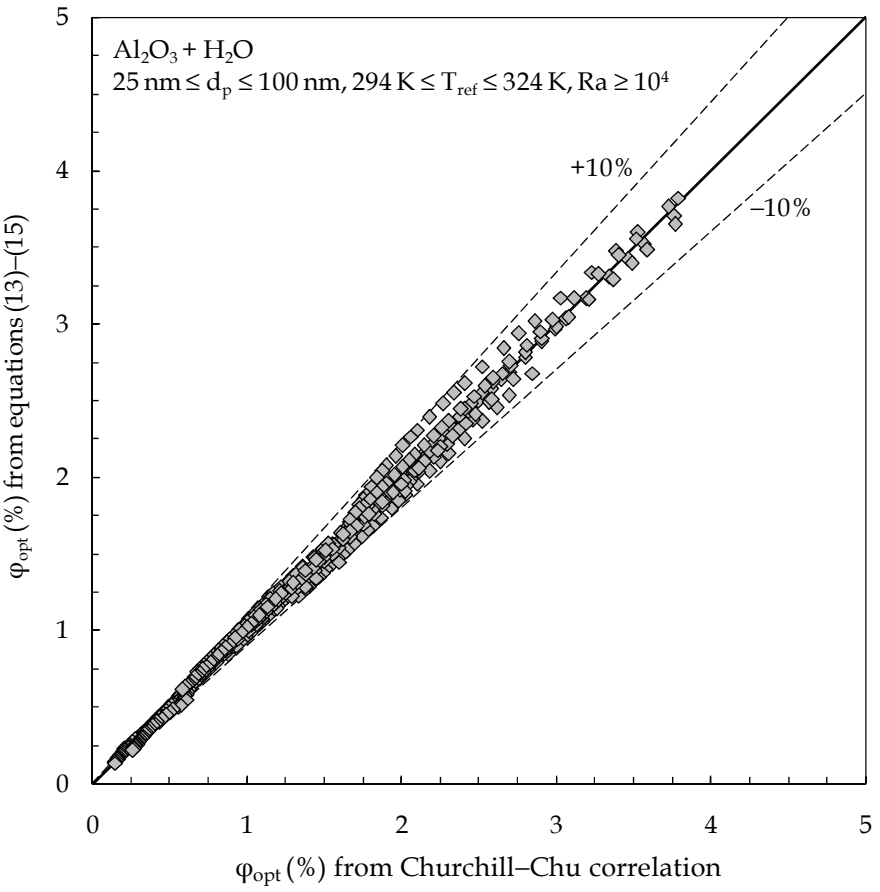

Figure 11: Comparison between eqs. (13)–(15) and the theoretical data of $\varphi_{opt}(\%)$.

thermal conductivity of ethylene glycol, the heat transfer enhancement produced by the addition of nanoparticles to the base liquid is less marked for water than for ethylene glycol.

For the specific case of a long horizontal isothermal cylinder suspended into Al_2O_3 + H_2O (that, according to the literature review, seems to be the nanofluid most frequently investigated), a multiple regression analysis of the results obtained for the percentage optimal particle loading φ_{opt} produces the following empirical dimensional algebraic equation:

$$\varphi_{opt}(\%) = \varphi_{opt-25}(\%) + [\varphi_{opt-100}(\%) - \varphi_{opt-25}(\%)] \times [d_p(nm) - 25]/75, \quad (13)$$

where

$$\varphi_{opt-25}(\%) = \{6.77889 \times Ln[t(^{\circ}C)] - 17.78553\} \times [\mathrm{Log}(Ra)]^{[0.01406 \times t(^{\circ}C) - 1.35790]} \quad (14)$$

$$\varphi_{opt-100}(\%) = \left\{0.00586 \times [t(^{\circ}C)]^{1.94286}\right\} \times [\mathrm{Log}(Ra)]^{\left\{0.00024 \times [t(^{\circ}C)]^2 - 0.00674 \times t(^{\circ}C) - 1.11677\right\}}. \quad (15)$$

The range of error of the above equation, in which d_p(nm) is the nanoparticle diameter in nm and t(°C) = $T_{ref} - 273.15$ is the average temperature of the nanofluid in degrees Celsius, is $\pm 10\%$, as shown in Fig. 11.

5 Conclusions

In the present paper, assumed that nanofluids behave more like a single-phase fluid rather than like a conventional solid-liquid mixture, the usually recommended Churchill−Chu correlation for single-phase natural convection around horizontal isothermal cylinders has been extended to nanoparticle suspensions by simply replacing the thermophysical properties appearing in it with the nanofluid effective properties calculated at the reference temperature. In particular, the effective mass density, specific heat at constant pressure and coefficient of thermal expansion of the nanofluid have been computed by the traditional mixing theory. On the contrary, the effective thermal conductivity and dynamic viscosity have been evaluated through a pair of empirical equations, that, without pretending to explain the physics behind the thermal and rheological behavior of nanofluids, were produced with the specific aim to obtain faithful interpolations of a sufficiently wide number of experimental data available in the literature, and use them only for theoretical investigation purposes. The percentage heat transfer enhancement deriving from the dispersion of solid nanoparticles into a pure liquid has been calculated for average temperatures of the nanofluid in the range between 294 K and 324 K, nanoparticle diameters in the range between 25 nm and 100 nm, and Rayleigh numbers of the base fluid up to 10^{13}, as well as for three different nanoparticle materials (i.e. Al_2O_3, CuO, and TiO_2) and two different base fluids (i.e. water and ethylene glycol).

The main results obtained may be summarized as follows:

1. The heat transfer enhancement increases with increasing the nanoparticle volume fraction up to an optimal particle loading; excessive increases of the

volume fraction above the optimal value may bring to remarkable deteriorations of the heat transfer rate at the cylinder surface with respect to the base case of pure host liquid.

2. The optimal particle loading, and the corresponding maximum heat transfer enhancement, increase as the average temperature of the nanofluid increases, and the size of the suspended nanoparticles decreases.

3. The heat transfer enhancement is much more remarkable at small Rayleigh numbers rather than at large Rayleigh numbers of the base fluid.

4. When different nanofluids are considered, the heat transfer enhancement and the optimal particle loading depend much more by the base liquid than by the nanoparticle material.

5. Finally, for the case of alumina nanoparticles dispersed into pure water, an empirical dimensional algebraic equation has been developed for the evaluation of the optimal particle loading at which the relative heat transfer performance has a peak.

References

Bejan, A. (2004): *Convection Heat Transfer*, 3rd ed., John Wiley & Sons, Inc., Hoboken, New Jersey, p. 221.

Brinkman, H. C. (1952): The viscosity of concentrated suspensions and solutions. *J. Chem. Phys.*, vol. 20, pp. 571.

Bruggemann, D. A. G. (1935): Berechnung Verschiedener Physikalischer Konstanten von Heterogenen Substanzen, I. Dielektrizitatskonstanten und Leitfahigkeiten der Mischkorper aus Isotropen Substanzen. *Ann. Phys.*, vol. 24, pp. 636-679.

Buongiorno, J.; et al. (2009): A benchmark study on the thermal conductivity of nanofluids. *J. Appl. Phys.*, vol. 106, paper No. 094319.

Chen, H.; Ding, Y.; Tan, C. (2007): Rheological behaviour of nanofluids. *New Journal of Physics*, vol. 9, paper No. 367.

Chen, H.; Ding, Y.; He, Y.; Tan, C. (2007): Rheological behaviour of ethylene glycol based titania nanofluids. *Chem. Phys. Lett.*, vol. 444, pp. 333-337.

Chevalier, J.; Tillement, O.; Ayela, F. (2007): Rheological properties of nanofluids flowing through microchannels. *Appl. Phys. Lett.*, vol. 91, paper No. 233103.

Chon, C. H.; Kihm, K. D. (2005): Thermal conductivity enhancement of nanofluids by Brownian motion. *J. Heat Transfer*, vol. 127, p. 810.

Chon, C. H.; Kihm, K. D.; Lee, S. P.; Choi, S. U. S. (2005): Empirical correlation finding the role of temperature and particle size for nanofluid (Al_2O_3) thermal conductivity enhancement. *Appl. Phys. Lett.*, vol. 87, paper No. 153107.

Churchill, S. W.; Chu, H. H. S. (1975): Correlating equations for laminar and turbulent free convection from a horizontal cylinder. *Int. J. Heat Mass Transfer*, vol.18, pp. 1049-1053.

Corcione, M. (2010): Heat transfer features of buoyancy-driven nanofluids inside rectangular enclosures differentially heated at the sidewalls. *Int. J. Thermal Sciences*, vol. 49, pp. 1536-1546.

Das, S. K.; Putra, N.; Roetzel, W. (2003): Pool boiling characteristics of nanofluids. *Int. J. Heat Mass Transfer*, vol. 46, pp. 851-862.

Das, S. K.; Putra, N.; Thiesen, P.; Roetzel, W. (2003): Temperature dependence of thermal conductivity enhancement for nanofluids. *J. Heat Transfer*, vol. 125, pp. 567-574.

Daungthongsuk, W.; Wongwises, S. (2007): A critical review of convective heat transfer in nanofluids. *Renewable Sustainable Energy Rev.*, vol. 11, pp. 797-817.

Duangthongsuk, W.; Wongwises, S. (2009): Measurement of temperature-dependent thermal conductivity and viscosity of TiO_2-water nanofluids. *Exp. Thermal Fluid Sciences*, vol. 33, pp. 706-714.

Eapen, J.; Williams, W. C.; Buongiorno, J.; Hu, L.-W.; Yip, S.; Rusconi, R.; Piazza, R. (2007): Mean-field versus microconvection effects in nanofluid thermal conduction. *Phys. Rev. Lett.*, vol. 99, paper No. 095901.

Eastman, J. A.; Choi, S. U. S.; Li, S.; Yu, W.; Thompson, L. J. (2001): Anomalously increased effective thermal conductivity of ethylene glycol-based nanofluids containing copper nanoparticles. *Appl. Phys. Lett.*, vol. 78, pp. 718-720.

Einstein, A. (1906): Eine neue Bestimmung der Molekuldimension. *Ann. Phys.*, vol. 19, pp. 289-306.

Einstein, A. (1911): Berichtigung zu meiner Arbeit: Eine neue Bestimmung der Molekuldimension. *Ann. Phys.*, vol. 34, pp. 591-592.

El Alami, M.; Semma E. A.; Najam M.; Boutarfa R (2009): Numerical study of convective heat transfer in a horizontal channel. *FDMP: Fluid Dynamics & Materials Processing*, vol. 5, pp. 23-36.

Evans, W.; Prasher, R.; Fish, J.; Meakin, P.; Phelan, P.; Keblinski, P. (2008): Effect of aggregation and interfacial thermal resistance on thermal conductivity of nanocomposites and colloidal nanofluids. *Int. J. Heat Mass Transfer*, vol. 51, pp. 1431-1438.

Ganguly, S.; Chakraborty S. (2009): Effective viscosity of nanoscale colloidal

suspensions. *J. Appl. Phys.*, vol. 106, paper No. 124309.

Garg, J.; Poudel, B.; Chiesa, M.; Gordon, J. B.; Ma, J. J.; Wang, J. B.; Ren, Z. F.; Kang, Y. T.; Ohtani, H.; Nanda, J.; McKinley, G. H.; Chen, G. (2008): Enhanced thermal conductivity and viscosity of copper nanoparticles in ethylene glycol nanofluid. *J. Appl. Phys.*, vol. 103, paper No. 074301.

Hamilton, R. L.; Crosser, O. K. (1962): Thermal conductivity of heterogeneous two component systems. *Ind. Eng. Chem. Fundam.*, vol. 1, pp. 187-191.

He, Y.; Jin, Y.; Chen, H.; Ding, Y.; Cang, D.; Lu, H. (2007): Heat transfer and flow behaviour of aqueous suspensions of TiO_2 nanoparticles (nanofluids) flowing upward through a vertical pipe. *Int. J. Heat Mass Transfer*, vol. 50, pp. 2272-2281.

Hwang, K. S.; Lee, J.-H.; Jang, S. P. (2007): Buoyancy-driven heat transfer of water-based Al_2O_3 nanofluids in a rectangular cavity. *Int. J. Heat Mass Transfer*, vol. 50, pp. 4003-4010.

Incropera, F. P.; DeWitt, D. P.; Bergman, T. L.; Lavine, A. S. (2007): *Fundamentals of Heat and Mass Transfer*, 6^{th} ed., John Wiley & Sons, Inc., Hoboken, New Jersey, p. 580.

Jang, S. P.; Choi, S. U. S. (2004): Role of Brownian motion in the enhanced thermal conductivity of nanofluids. *Appl. Phys. Lett.*, vol. 84, pp. 4316-4318.

Kakaç, S.; Pramuanjaroenkij, A. (2009): Review of convective heat transfer enhancement with nanofluid. *Int. J. Heat Mass Transfer*, vol. 52, pp. 3187-3196.

Keblinski, P.; Phillpot, S. R.; Choi, S. U. S.; Eastman, J. A. (2002): Mechanisms of heat flow in suspensions of nano-sized particles (nanofluids). *Int. J. Heat Mass Transfer*, vol. 45, pp. 855-863.

Kim, J; Kang, Y. T.; Choi, C. K. (2004): Analysis of convective instability and heat transfer characteristics of nanofluids. *Phys. Fluids*, vol. 16, pp. 2395-2401.

Koo, J. (2005): *Computational nanofluid flow and heat transfer analyses applied to micro-systems*, Dissertation Thesis, North Carolina State University, Rayleigh, NC.

Koo, J.; Kleinstreuer, C. (2004): A new thermal conductivity model for nanofluids. *J. Nanopart. Res.*, vol. 6, pp. 577-588.

Kumar, D. H.; Patel, H. E.; Kumar, V. R. R.; Sundararajan, T.; Pradeep, T.; Das, S. K. (2004): Model for heat conduction in nanofluids. *Phys. Rev. Lett.*, vol 93, paper No. 144301.

Lee, J.-H.; Hwang, K. S.; Jang, S. P.; Lee, B. H.; Kim, J. H.; Choi, S. U. S.; Choi, C. J. (2008): Effective viscosities and thermal conductivities of aqueous nanofluids containing low volume concentrations of Al_2O_3 nanoparticles. *Int. J. Heat Mass Transfer*, vol. 51, pp. 2651-2656.

Lee, S.; Choi, S. U. S.; Li, S.; Eastman, J. A. (1999): Measuring thermal conductivity of fluids containing oxide nanoparticles. *J. Heat Transfer*, vol. 121, pp. 280-289.

Leong, K. C.; Yang, C.; Murshed, S. M. S. (2006): A model for the thermal conductivity of nanofluids – the effect of interfacial layer. *J. Nanopart. Res.*, vol. 8, pp. 245-254.

Li, C. H.; Peterson, G. P. (2006): Experimental investigation of temperature and volume fraction variations on the effective thermal conductivity of nanoparticle suspensions (nanofluids). *J. Appl. Phys.*, vol. 99, paper No. 084314.

Martynenko, O. G.; Khramtsov, P. P. (2005): *Free-Convective Heat Transfer*, Springer-Verlag, Berlin, p. 234.

Masoumi, N.; Sohrabi, N.; Behzadmehr, A. (2009): A new model for calculating the effective viscosity of nanofluids. *J. Phys. D: Appl. Phys.*, vol. 42, paper No. 055501.

Masuda, H.; Ebata, A.; Teramae, K.; Hishinuma, N. (1993): Alteration of thermal conductivity and viscosity of liquid by dispersing ultra-fine particles (dispersion of γ-Al_2O_3, SiO_2, and TiO_2 ultra-fine particles). *Netsu Bussei*, vol. 4, pp. 227-233.

Maxwell-Garnett, J. C. (1904): Colours in metal glasses and in metallic films. *Philos. Trans. Roy. Soc. A*, vol. 203, pp. 385-420.

Meskini A.; Najam M.; El Alami M.: Convective mixed heat transfer in a square cavity with heated rectangular blocks and submitted to a vertical forced flow. *FDMP: Fluid Dynamics & Materials Processing*, vol. 7 no. 1, pp. 97-110.

Mintsa, H. A.; Roy, G.; Nguyen, C. T.; Doucet, D. (2009): New temperature dependent thermal conductivity data for water-based nanofluids. *Int. J. Thermal Sciences*, vol. 48, pp. 363-371.

Murshed, S. M. S.; Leong, K. C.; Yang, C. (2008a): Thermophysical and electrokinetic properties of nanofluids – A critical review. *Applied Thermal Eng.*, vol. 28, pp. 2109-2125.

Murshed, S. M. S.; Leong, K. C.; Yang, C. (2008b): Investigations of thermal conductivity and viscosity of nanofluids. *Int. J. Thermal Sciences*, vol. 47, pp. 560-568.

Murshed, S. M. S.; Leong, K. C.; Yang, C. (2009): A combined model for the effective thermal conductivity of nanofluids. *Appl. Thermal Eng.*, vol. 29, pp. 2477-2483.

Pak, B. C.; Cho, Y. I. (1998): Hydrodynamic and heat transfer study of dispersed fluids with submicron metallic oxide particles. *Exp. Heat Transfer*, vol. 11, pp.

151-170.

Patel, H. E.; Sundararajan, T.; Pradeep, T.; Dasgupta, A.; Dasgupta, N.; Das, S. K. (2005): A micro-convection model for the thermal conductivity of nanofluids. *Pramana – J. Phys.*, vol. 65, pp. 863-869.

Prakash, M.; Giannelis, E. P. (2007): Mechanism of heat transport in nanofluids. *J. Computer-Aided Mater. Des.*, vol. 14, pp. 109-117.

Prasher, R.; Bhattacharya, P.; Phelan, P. E. (2005): Thermal conductivity of nanoscale colloidal solutions (nanofluids). *Phys. Rev. Lett.*, vol. 94, paper No. 025901.

Prasher, R.; Bhattacharya, P.; Phelan, P. E. (2006): Brownian motion-based convective-conductive model for the effective thermal conductivity of nanofluids. *J. Heat Transfer*, vol. 128, pp. 588-595.

Prasher, R.; Evans, W.; Meakin, P.; Fish, J.; Phelan, P.; Keblinski, P. (2006): Effect of aggregation on thermal conduction in colloidal nanofluids. *Appl. Phys. Lett.*, vol. 89, paper No. 143119.

Prasher, R.; Phelan, P. E.; Bhattacharya, P. (2006): Effect of aggregation kinetics on the thermal conductivity of nanoscale colloidal solutions (nanofluid). *Nano Letters*, vol. 6, pp. 1529-1534.

Prasher, R.; Song, D.; Wang, J.; Phelan, P. (2006): Measurements of nanofluid viscosity and its implications for thermal applications. *Appl. Phys. Lett.*, vol. 89, paper No. 133108.

Putra, N.; Roetzel, W.; Das, S. K. (2003): Natural convection of nano-fluids. *Heat Mass Transfer*, vol. 39, pp. 775-784.

Ren, Y.; Xie, H.; Cai, A. (2005): Effective thermal conductivity of nanofluids containing spherical nanoparticles. *J. Phys. D: Appl. Phys.*, vol. 38, pp. 3958-3961.

Wang, B.-X.; Zhou, L.-P.; Peng, X.-F. (2003): A fractal model for predicting the effective thermal conductivity of liquid with suspension of nanoparticles. *Int. J. Heat Mass Transfer*, vol. 46, pp. 2665-2672.

Wang, X.; Xu, X.; Choi, S. U. S. (1999): Thermal conductivity of nanoparticle-fluid mixture. *J. Thermophys. Heat Transfer*, vol. 13, pp. 474-480.

Xie, H.; Fujii, M.; Zhang, X. (2005): Effect of interfacial nanolayer on the effective thermal conductivity of nanoparticle-fluid mixture. *Int. J. Heat Mass Transfer*, vol. 48, pp. 2926-2932.

Xuan, Y.; Li, Q.; Hu, W. (2003): Aggregation structure and thermal conductivity of nanofluids. *AIChE J.*, vol. 49, pp.1038-1043.

Xuan, Y.; Li, Q.; Zhang, X.; Fujii, M. (2006): Stochastic thermal transport of nanoparticle suspensions. *J. Appl. Phys.*, vol. 100, paper No. 043507.

Xue, Q.-Z. (2003): Model for effective thermal conductivity of nanofluids. *Phys. Lett. A*, vol. 307, pp. 313-317.

Yu, W.; Choi, S. U. S. (2003): The role of interfacial layers in the enhanced thermal conductivity of nanofluids: a renovated Maxwell model. *J. Nanopart. Res.*, vol. 5, pp. 167-171.

Yu, W.; Xie, H.; Chen, L.; Li, Y. (2010): Investigation on the thermal transport properties of ethylene glycol-based nanofluids containing copper nanoparticles. *Powder Tecnology*, vol. 197, pp. 218-221.